

Theoretical analysis of mechanical displacement measurement using a multiple cavity mode transducer

J.M. Dobrindt¹ and T.J. Kippenberg^{1,2,*}

¹Max Planck Institut für Quantenoptik, D-85748 Garching, Germany

²Ecole Polytechnique Fédérale de Lausanne (EPFL), CH-1015 Lausanne, Switzerland

We present an optomechanical displacement transducer, that relies on three cavity modes parametrically coupled to a mechanical oscillator and whose frequency spacing matches the mechanical resonance frequency. The additional resonances allow to reach the standard quantum limit at substantially lower input power (compared to the case of only one resonance), as both, sensitivity and quantum backaction are enhanced. Furthermore, it is shown that in the case of multiple cavity modes, coupling between the modes is induced via reservoir interaction, e.g., enabling quantum backaction noise cancellation. Experimental implementation of the schemes is discussed in both the optical and microwave domain.

PACS numbers: 42.60.Da, 42.81.Qb

Introduction.— High frequency nano- and micro-mechanical oscillators have received a high degree of attention recently. They have been used as sensitive detectors, e.g. for spin [1] or particle mass [2], but also carry an intrinsic interest in the study of small scale dissipation of mechanical systems [3], quantum limited motion detection [18], and backaction cooling of vibrational modes [4]. These studies have in common that a sensitive motion transduction is required, which can be implemented by parametric coupling to an optical, electrical, or microwave resonator. The ideal transducer should i) have a high sensitivity and possibly operate at the standard quantum limit (SQL), and ii) should operate at low power. The latter is experimentally advantageous, as high power may cause excess heating due to intrinsic losses. The former pertains to the minimum uncertainty in motion detection and arises from the trade off between measurement imprecision, inherent to the meter (i.e., detector shot noise), and (for linear continuous measurements) inevitable *quantum backaction* (QBA) [5, 6]. These processes are characterized by the displacement spectral density $\bar{S}_{xx}(\Omega)$ and the QBA force spectral density $\bar{S}_{FF}(\Omega)$ [28]. For a parametric motion transducer, where a single cavity mode (with frequency ω_0 and energy decay rate κ) is parametrically coupled to a mechanical oscillator [7], the spectral densities are given by

$$\begin{aligned}\bar{S}_{xx}(\Omega) &= \frac{\kappa^2 \hbar \omega_0}{64 G^2 P} \left(1 + \frac{4\Omega^2}{\kappa^2} \right) \\ \bar{S}_{FF}(\Omega) &= \frac{16 \hbar G^2 P}{\kappa^2 \omega_0} \left(1 + \frac{4\Omega^2}{\kappa^2} \right)^{-1}.\end{aligned}\quad (1)$$

Here P is the input power and the optomechanical coupling strength is determined by the cavity frequency shift due to mechanical displacement: $G = \frac{d\omega_0}{dx}$. Equations 1 satisfy $\sqrt{\bar{S}_{xx}[\Omega] \bar{S}_{FF}[\Omega]} \geq \hbar/2$, which is a consequence of the Heisenberg uncertainty principle [8]. The canonical way to lower the power to reach the SQL is to increase the cavity finesse, i.e., decreasing κ . However,

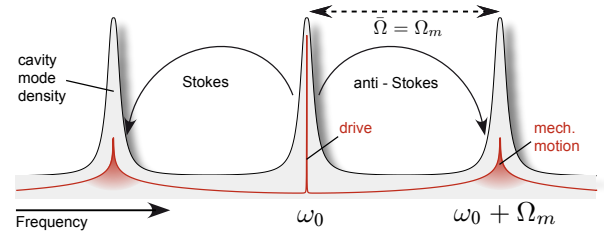


Figure 1: Illustration of the triple mode transducer scheme. Auxiliary cavity resonances at $\omega_0 \pm \Omega_m$ permit resonant motional side band build-up.

Eqs. 1 reveals a fundamental deficiency: decreasing κ for fixed P only improves readout sensitivity as long as the mechanical signal (frequency Ω_m) lies within the cavity bandwidth, i.e., $\Omega_m < \kappa$, while for $\Omega_m > \kappa$ the displacement sensitivity experiences saturation. Physically this phenomenon is readily understood; the mechanical motion modulates the cavity field and creates motional sidebands at $\omega_0 \pm \Omega_m$, which constitute the readout signal. For $\kappa \ll \Omega_m$, i.e., in the resolved sideband regime (RSB), the sidebands (and therefore the signal) are suppressed. This regime has recently been subject to experimental investigation [17, 18].

Here we present a readout scheme where this fundamental limitation is overcome, by placing two auxiliary cavity resonances at $\omega_0 \pm \Omega_m$ around the central, driven resonance [cf. Fig. 1]. This enables resonant side band build-up and causes a substantial decrease in the power required to reach the SQL. Moreover, we show that this scheme, when applied to the case of two resonances, can lead to quantum backaction interference, without the requirement of having a dissipative parametric coupling [9].

Theoretical model.— In this section we present the theoretical framework, to describe multiple cavity modes parametrically coupled to a mechanical degree of freedom, described by its frequency Ω_m and effective mass m_{eff} . This model covers a wide range of experimental im-

plementations on both nano- and microscale, as well as in the optical and electrical domain. The cavity features several equidistant modes at frequencies $\omega_k = \omega_0 + k \cdot \bar{\Omega}$ ($k \in \mathbb{Z}$), described by the annihilation(creation) operators \hat{a}_k (\hat{a}_k^\dagger), where $\bar{\Omega}$ denotes the spacing between adjacent modes. A driving field at frequency ω_0 (input power P) is coupled to the central cavity mode. Furthermore the optical modes are parametrically coupled to the mechanical degree of freedom, \hat{a}_m (\hat{a}_m^\dagger) and zero point motion $x_0 = \sqrt{\hbar/2m_{\text{eff}}\bar{\Omega}_m}$, via the interaction Hamiltonian [10]

$$\hat{H}_{\text{int}} = \hbar x_0 \sum_{k,l} G \hat{a}_k^\dagger \hat{a}_l (\hat{a}_m + \hat{a}_m^\dagger). \quad (2)$$

The geometric factor, coming from the mode overlap integral, is assumed (for simplicity) to be unity. Cavity damping is modeled by coupling the cavity modes to a harmonic oscillator bath via the damping Hamiltonian

$$\hat{H}_{\text{damp}} = i\hbar \sum_k \int_{-\infty}^{+\infty} d\omega \left[g_k^*(\omega) \hat{b}_\omega \hat{a}_k^\dagger - g_k(\omega) \hat{a}_k \hat{b}_\omega^\dagger \right]. \quad (3)$$

The bath operators obey the commutation relations $[\hat{b}_\omega, \hat{b}_{\omega'}^\dagger] = \delta(\omega - \omega')$. In the following we will consider a classical harmonic oscillator characterized by the position $\hat{q} = x_0(\hat{a}_m + \hat{a}_m^\dagger)$ and damping rate γ_m . This treatment is justified, as we are solely interested in the transduction properties of the cavity, and the quantum backaction coming from the quantized nature of the field.

We eliminate the bath in the Markovian limit [11] setting $g_k(\omega) = \sqrt{\kappa}$. Surprisingly the damping Hamiltonian does not only couple the cavity modes to the dissipative bath, but also couples the modes among each other via the reservoir dynamics [cf. Eqs. 4]. This off-resonant interaction is well known in laser theory (where it is responsible for Petermann excess noise [12]), but has (to the authors knowledge) never been applied to the context of opto- or electromechanics.

In the next step, we derive the Heisenberg-Langevin equations (HLE) for the optical modes, where the classical drive is eliminated by moving to a rotating frame at the drive frequency and subsequently transforming to the general quadrature fluctuations $\hat{X}_{k,\theta} \equiv e^{-i\theta}(\hat{a}_k - \langle \hat{a}_k \rangle) + e^{i\theta}(\hat{a}_k^\dagger - \langle \hat{a}_k^\dagger \rangle)$. We emphasize, that choosing one global rotating frame for all modes is essential, as it enables us to treat off-resonant interaction terms (to first order). These are known to account for quantum limits [13]. Explicitly the linearized HLE for the canonical quadrature fluctuations $\hat{X}_k = \hat{X}_{k,\theta=0}$ and $\hat{Y}_k = \hat{X}_{k,\theta=\pi/2}$ are

$$\begin{aligned} \dot{\hat{X}}_k &= -k \cdot \bar{\Omega} \hat{Y}_k - \frac{\kappa}{2} \sum_l \hat{X}_l + \sqrt{\kappa} \delta \hat{X}^{\text{in}}[t] \\ \dot{\hat{Y}}_k &= k \cdot \bar{\Omega} \hat{X}_k - \frac{\kappa}{2} \sum_l \hat{Y}_l + g_m \hat{q}[t]/x_0 + \sqrt{\kappa} \delta \hat{Y}^{\text{in}}[t] \\ \ddot{\hat{q}} &= -\gamma_m \dot{\hat{q}} - \Omega_m^2 \hat{q} + x_0 g_m \sum_l \hat{X}_l. \end{aligned} \quad (4)$$

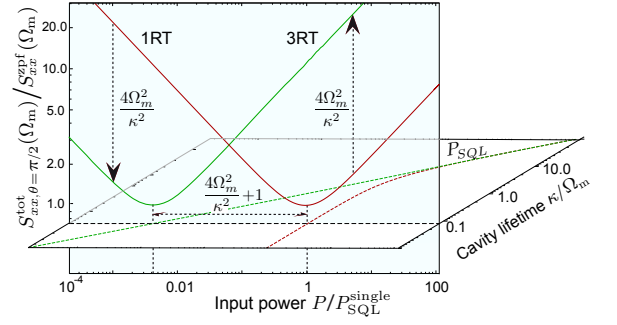


Figure 2: The measurement noise spectrum $S_{xx,\theta=\pi/2}^{\text{tot}}(\Omega_m)$ (normalized to $S_{xx}^{\text{zpf}}(\Omega_m) = \hbar|\chi_0(\Omega_m)|$) for the triple cavity mode transducer as a function of the input power (with $\kappa = \Omega_m/10$) compared to the single mode case. The traces in the horizontal plane follow the minima as a function of the cavity life time κ^{-1} .

Solving for the canonical quadratures allows us to transform to the θ -dependent general quadrature. The global phase of the input field is chosen in the way that $\bar{\alpha} = \Sigma \langle \hat{a}_j \rangle$ and the optomechanical coupling rate $g_m = 2Gx_0\bar{\alpha}$ are real[29]. The noise operators in the HLE are δ -correlated: $\langle \delta \hat{X}^{\text{in}}[t] \delta \hat{X}^{\text{in}}[t'] \rangle = \langle \delta \hat{Y}^{\text{in}}[t] \delta \hat{Y}^{\text{in}}[t'] \rangle = \delta(t - t')$, $\langle \delta \hat{X}^{\text{in}}[t] \delta \hat{Y}^{\text{in}}[t'] \rangle = \langle \delta \hat{Y}^{\text{in}}[t] \delta \hat{X}^{\text{in}}[t'] \rangle^* = i\delta(t - t')$. We can account for intrinsic cavity loss by introducing a second loss channel in Eqs. 4, characterized by the internal loss rate κ_0 . It will appear in the results as the degree of overcoupling $\eta_c = \kappa_0/\kappa_{\text{tot}}$, with κ_{tot} being the total cavity decay rate[30]. For multiple cavity modes, the output quadrature fluctuations are given by a generalized input-output relation [14]

$$\hat{X}_\theta^{\text{out}} + \hat{X}_\theta^{\text{in}} = \sqrt{\kappa} \sum_k \hat{X}_{k,\theta} \quad (5)$$

Triple mode transducer.— Having introduced the theoretical model, we calculate the output spectrum of a cavity with three optical modes, spaced by the mechanical resonance frequency, i.e. $\bar{\Omega} = \Omega_m$. When the central resonance is driven, side bands at $\omega_0 \pm \Omega_m$, that encode for the mechanical motion, build up efficiently [cf. Fig. 1] and signal to noise is enhanced.

From Eqs. 4 we calculate the quadrature fluctuations in Fourier space. Using the multimode input-output relation (Eq. 5), the spectrum of the output fluctuations is derived. Importantly the off-resonant reservoir coupling terms ($\propto \kappa/2$ in Eqs. 4) preserve a flat shot noise spectrum for the decoupled ($g_m = 0$) cavity. The measurement noise spectrum $S_{xx,\theta}^{\text{tot}}(\Omega) = S_{xx,\theta}(\Omega) + |\chi_0(\Omega)|^2 S_{FF}(\Omega)$ is obtained by scaling the output fluctuations to the mechanical signal [15]. The classical motion of the mechanical oscillator, characterized by its bare susceptibility $\chi_0(\Omega)$, is not affected by the coupling, as dynamical backaction effects are absent

[16]. The shot noise background is given by

$$S_{xx,\theta}^{\text{triple}}(\Omega) = \frac{1}{\sin^2 \theta} \frac{x_0^2 \kappa}{\eta_c g_m^2} \left(1 + \frac{4\Omega^2 (\Omega_m^2 - \Omega^2)^2}{\kappa^2 (\Omega_m^2 - 3\Omega^2)^2} \right). \quad (6)$$

The sensitivity is maximized for $\theta = \pi/2$, implying that the information on the mechanical signal is encoded in the phase quadrature. Comparing $S_{xx,\theta}^{\text{triple}}(\Omega)$ to the single resonance transducer, we note that the transduction properties of a low frequency signal remain unchanged, i.e., $S_{xx,\theta}^{\text{single}}(0)/S_{xx,\theta}^{\text{triple}}(0) = 1$. However the sensitivity at the mechanical resonance frequency is dramatically increased

$$S_{xx,\theta}^{\text{single}}(\Omega_m)/S_{xx,\theta}^{\text{triple}}(\Omega_m) = 1 + \frac{4\Omega_m^2}{\kappa^2}. \quad (7)$$

For systems that operate well into the RSB regime, such as toroidal microresonators [17] or superconducting microwave resonators [18], this factor is more than $\times 100$ and thus represents a major reduction. Based on the Heisenberg uncertainty principle for continuous position measurements, one expects that the enhanced sensitivity also implies an increased quantum backaction force spectral density. Physically these can be viewed as the beat of the carrier (at ω_0) with vacuum fluctuations at $\omega_0 + \Omega_m$, which resonantly heat the mechanical oscillator. The radiation pressure force fluctuations are given by

$$\delta \hat{F}^{\text{rP}}[\Omega] = \frac{\hbar g_m}{2x_0} \sum_k \hat{X}_k[\Omega]. \quad (8)$$

Indeed, in the same way, that the shot noise is reduced, the backaction force spectral density $S_{FF}^{\text{triple}}(\Omega)$ is increased, and the Heisenberg limit of the single resonance transducer is recovered.

$$\sqrt{\overline{S_{xx,\theta=\pi/2}^{\text{triple}}(\Omega)} \cdot \overline{S_{FF}^{\text{triple}}(\Omega)}} = \frac{\hbar}{2\sqrt{\eta_c}}. \quad (9)$$

We emphasize that the recovery of the Heisenberg limit is a consequence of the off-resonant coupling. Moreover, the triple transducer has the significant advantage over a single cavity mode transducer that the SQL is reached at substantially lower power: $P_{\text{SQL}}^{\text{single}}/P_{\text{SQL}}^{\text{triple}} \approx 4\Omega_m^2/\kappa^2$ [31]. Moreover, the enhanced QBA itself can be a valuable resource. Indeed, many quantum optomechanical experiments rely on QBA to be the dominant force noise, such as in experiments relating to ponderomotive squeezing [19] or two beam entanglement [20].

Dual mode scheme.— Within the framework of the multimode transducer theory, we can also consider the situation of two resonances, spaced by the mechanical resonance frequency [21, 22]. The situation differs from the triple mode scheme, as only the anti-Stokes process is resonantly enhanced by pumping the lower frequency mode. This results in net cooling of the mechanical degree of freedom, because every scattering process annihilates one phonon[32]. Then the response to an external

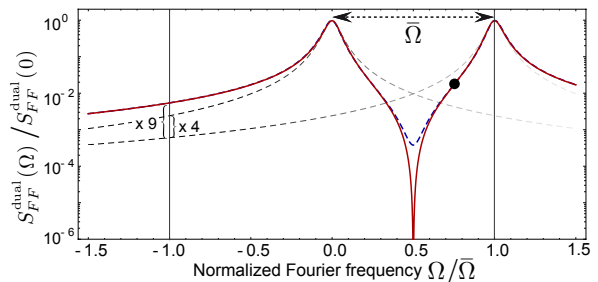


Figure 3: The normalized quantum backaction force spectral density $S_{FF}^{\text{dual}}(\Omega)/S_{FF}^{\text{dual}}(+\Omega_m)$ (thick solid line) is plotted together with the result from a classical model (thick dashed line). The reservoir interaction between the modes leads to complete noise cancellation at $\Omega = \Omega_m/2$. The thin dashed lines indicate the backaction force coming from two uncorrelated modes.

force, e.g. a thermal Langevin force, a signal force, or quantum Langevin forces, is suppressed as a result of the damped mechanical motion. Consequently the transduction properties are not ideal.

Next, we calculate the QBA spectral density from Eq. 8.

$$S_{FF}^{\text{dual}}(\Omega) = \frac{\hbar^2}{x_0^2} \frac{g_m^2 \kappa (\Omega_m - 2\Omega)^2}{4(\Omega_m - \Omega)^2 \Omega^2 + \kappa^2 (\Omega_m - 2\Omega)^2} \quad (10)$$

Then an estimate for the final occupancy of the mechanical mode $n_f = \langle \hat{a}_m^\dagger \hat{a}_m \rangle$ is given by the quantum noise approach [6]. Unexpectedly, compared to the single resonance dynamical backaction cooling [23, 24], the quantum limit increases by a factor of $\times 9$.

$$\frac{n_f}{n_f + 1} = \frac{S_{FF}^{\text{dual}}(-\Omega_m)}{S_{FF}^{\text{dual}}(+\Omega_m)}, \Rightarrow n_f \approx 9 \frac{\kappa^2}{16\Omega_m^2} \quad (11)$$

This is understood from the constructive quantum noise interference at $\Omega = -\Omega_m$ [cf. Fig 3, $(\sqrt{1} + \sqrt{4})^2 = 9$]. However, the QBA spectrum in Fig. 3 reveals an additional, striking feature. At $\Omega = \Omega_m/2$ the *quantum noise exactly cancels*. This is a direct consequence of the reservoir coupling terms in Eqs. 4. Omitting these terms yields a *classical* interference pattern, shown by the thick dashed curve in Fig. 3. The shape of the QBA spectrum suggests to tune the mode spacing to $\bar{\Omega} = 4\Omega_m$ and drive the cavity on the red wing of the upper resonance [cf. Fig. 3, black circle]. Then the heating term vanishes, i.e., $S_{FF}^{\text{dual}}(-\Omega_m) = 0$ (in the rotating frame). However, an exact analysis, using a covariance approach [25], reveals that finite line width effects lead to a power dependent quantum limit, i.e. $n_f \approx 2g_m^2/\Omega_m^2$. As the cooling rate saturates, when g_m approaches $\kappa/2$, one can find an upper limit for n_f by assuming $g_m < \kappa/2$ [13]. The same analysis for the canonical two mode cooling yields $n_f \approx (9\kappa^2 + 14g_m^2)/16\Omega_m^2$.

With respect to the transduction properties of the dual scheme we note, that in cooling experiments the QBA

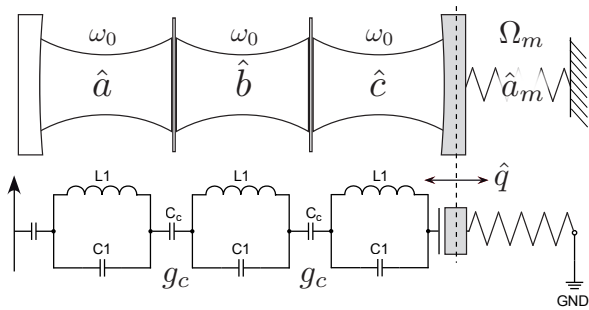


Figure 4: a) Three degenerate optical modes are coupled via semi-transparent mirrors. b) Three LC-oscillators (possibly microwave resonators) are capacitively coupled “in series”. While mode \hat{a} is connected to an external drive, i.e., a transmission line, mode \hat{c} is parametrically coupled to a mechanical oscillator. When the coupling rate $g_c > \kappa$ exceeds the individual decay rate, the spectrum exhibits normal mode splitting.

is not viewed as additional measurement noise (as for the 3RT), but contributes the signal itself. This is corroborated in the case of ground state cooling, where the field fluctuations conserve the zero point fluctuations of the mechanical oscillator, independently of its quantum nature.

Experimental implementation.— The experimental challenge in the design of a multimode transducer lies in matching the cavity mode spacing with the resonance frequency of the mechanical oscillator without adding additional damping. The canonical setup is a Fabry-Pérot cavity where the free spectral range matches the resonance frequency of the harmonically suspended back mirror. However difficulties might arise from differing mode overlap integrals. These challenges can be circumvented in a more general way, adaptable to optical, electrical, and microwave domain. As illustrated in Fig. 4, three degenerate cavity modes $\{\hat{a}, \hat{b}, \hat{c}\}$ are coupled *in series* via the linear interaction $\hbar g_c [\hat{b}(\hat{a}^\dagger + \hat{c}^\dagger) + \hat{b}^\dagger(\hat{a} + \hat{c})]$. In the microwave domain, this interaction can be realized by coupling of three superconducting quarter or half wave resonators (via inductive or capacitive coupling as shown in Fig. 4). In the optical domain, it can be achieved by coupling of degenerate cavity modes via partially transparent mirrors or evanescent field. In addition, only one mode (\hat{c}) is coupled to the mechanics by $\hat{H}_{\text{int}}^{\text{single}} = \hbar x_0 G \hat{c}^\dagger \hat{c} (\hat{a}_m + \hat{a}_m^\dagger)$. In the regime of strong mode coupling, when $g_c > \kappa$, the originally degenerate cavity modes exhibit normal mode splitting. The new cavity eigenmodes can then be represented in a basis of dressed states $\{\hat{a}_0, \hat{a}_+, \hat{a}_-\}$ with eigenfrequencies $\{\omega_0, \omega_0 \pm \sqrt{2}g_c\}$.

$$\begin{pmatrix} \hat{a}_0 \\ \hat{a}_- \\ \hat{a}_+ \end{pmatrix} \propto \begin{pmatrix} 0 & -1 & 1 \\ -1/\sqrt{2} & 1/2 & 1/2 \\ 1/\sqrt{2} & 1/2 & 1/2 \end{pmatrix} \cdot \begin{pmatrix} \hat{a} \\ \hat{b} \\ \hat{c} \end{pmatrix}. \quad (12)$$

The splitting $\sqrt{2}g_c$ can be matched to the mechanical resonance frequency by appropriately tuning the coupling rate. Transforming to the dressed state basis, one finds that the operator ($\hat{c} \propto \hat{a}_0 + \hat{a}_- + \hat{a}_+$) is proportional to the sum of the dressed state operators [cf. inverse of matrix in Eq. 12]. Replacing \hat{c} in the parametric interaction $\hat{H}_{\text{int}}^{\text{single}}$ results in a multimode interaction as given by Eq. 2. Indeed, a dual mode coupling of this kind has recently been demonstrated using toroidal microcavities [26] in this proposed way. Moreover, tunable mode splitting between counter propagating modes has also been achieved [27], making the experimental realization of this new class of high frequency transducers realistic. We acknowledge Warwick Bowen for discussion and making helpful and critical comments.

* Electronic address: tobias.kippenberg@epfl.ch

- [1] D. Rugar, R. Budakian, H. J. Mamin, and B. W. Chui, *Nature* **430**, 329 (2004), ISSN 0028-0836.
- [2] A. K. Naik, M. S. Hanay, W. K. Hiebert, X. L. Feng, and M. L. Roukes, *Nature Nanotech* **4**, 445 (2009).
- [3] G. A. Steele, A. K. Huttel, B. Witkamp, M. Poot, H. B. Meerwaldt, L. P. Kouwenhoven, and H. S. J. van der Zant, *Science* **325**, 1103 (2009).
- [4] T. J. Kippenberg and K. Vahala, *Science* **321**, 1172 (2008).
- [5] C. M. Caves, *Physical Review D* **26**, 1817 (1982).
- [6] A. A. Clerk, M. H. Devoret, S. M. Girvin, F. Marquardt, and R. J. Schoelkopf, 0810.4729 (2008).
- [7] V. B. Braginsky, *Measurement of Weak Forces in Physics Experiments* (University of Chicago Press, 1977).
- [8] V. B. Braginsky and F. Khalili, *Quantum Measurement* (Cambridge University Press, 1992).
- [9] F. Elste, S. M. Girvin, and A. A. Clerk, *Physical Review Letters* **102**, 207209 (2009).
- [10] C. K. Law, *Physical Review A* **51**, 2537 (1995).
- [11] C. W. Gardiner and P. Zoller, *Quantum Noise* (Springer, 2000).
- [12] A. E. Siegman, *Physical Review A* **39**, 1253 (1989).
- [13] J. M. Dobrindt, I. Wilson-Rae, and T. J. Kippenberg, *Physical Review Letters* **101**, 263602 (2008).
- [14] C. Viviescas and G. Hackenbroich, *Physical Review A* **67**, 013805 (2003).
- [15] M. Jaekel and S. Reynaud, *Europhysics Letters* **13**, 301 (1990).
- [16] W. Kells and E. D’Ambrosio, *Physics Letters A* **299**, 326 (2002).
- [17] A. Schliesser, R. Riviere, G. Anetsberger, O. Arcizet, and T. J. Kippenberg, *Nature Physics* **4**, 415 (2008).
- [18] J. D. Teufel, T. Donner, M. A. Castellanos-Beltran, J. W. Harlow, and K. W. Lehnert, 0906.1212 (2009).
- [19] P. Verlot, A. Tavernarakis, T. Briant, P. F. Cohadon, and A. Heidmann, arXiv:0809.2510 (2008).
- [20] S. Mancini, V. Giovannetti, D. Vitali, and P. Tombesi, *Physical Review Letters* **88**, 120401 (2002).
- [21] V. B. Braginsky, S. E. Strigin, and S. P. Vyatchanin, *Physics Letters A* **287**, 331 (2001).
- [22] A. B. Matsko, D. V. Strekalov, and N. Yu, *Physical Re-*

- view A (Atomic, Molecular, and Optical Physics) **77**, 043812 (2008).
- [23] F. Marquardt, J. P. Chen, A. A. Clerk, and S. M. Girvin, *Physical Review Letters* **99**, 093902 (2007).
- [24] I. Wilson-Rae, N. Nooshi, W. Zwerger, and T. J. Kippenberg, *Physical Review Letters* **99**, 093901 (2007).
- [25] I. Wilson-Rae, N. Nooshi, J. Dobrindt, T. J. Kippenberg, and W. Zwerger, *New Journal of Physics* **10**, 095007 (2008).
- [26] I. S. Grudinin, O. Painter, and K. J. Vahala, 0907.5212 (2009).
- [27] G. Anetsberger, O. Arcizet, Q. Unterreithmeier, E. Weig, J. Kotthaus, and T. Kippenberg, arXiv:0904.4051 .
- [28] The bar denotes a symmetrized spectral density: $\bar{S}(\Omega) = 1/2 (S(\Omega) + S(-\Omega))$.
- [29] This is always possible for a non-squeezed input field.
- [30] In the limit of overcoupling, $\eta_c \rightarrow 1$.
- [31] We note, that the mixing term $S_{xF,\theta}^{\text{triple}}(\Omega)$ is odd in Ω for $\theta = \pi/2$ and therefore disappears in the symmetrized spectrum.
- [32] On the other hand, pumping the higher frequency mode results in amplification.